Stochastic Diffusion of Energetic Ions Due to Incoherent Lower Hybrid Waves

Lucio M. Tozawa and Luiz F. Ziebell
Instituto de Física, Universidade Federal do Rio Grande do Sul
Caixa Postal 15051, 91501-970, Porto Alegre, RS, Brasil

Received on 9 May, 2003

In the present paper we discuss stochastic diffusion of energetic ions by a set of lower hybrid waves with frequencies close to each other and random phases which change along the time evolution of the system. We obtain efficient long term diffusion in velocity space, which is more representative of the diffusion produced by a continuous wave packet than the diffusion produced by a set of waves with random phases which are constant along the time evolution.

1 Introduction

It is known that the movement of ions in a uniform magnetic field may become stochastic in the presence of a coherent electrostatic wave, if the wave amplitude is sufficiently large [1, 2]. The ensuing diffusion in velocity space may have important consequences, as indicated by relatively recent experiments, which show evidence of interaction between lower hybrid waves and energetic ions in large tokamaks [3, 4]. A parametric analysis has shown that the threshold condition for stochasticity as derived in Ref. [1] is not easily satisfied in present day large tokamaks, although it can be attained in small tokamaks with relatively modest levels of wave power [5]. When the threshold condition is satisfied a quasilinear formalism can be derived and employed to describe the stochastic diffusion which occurs in velocity space [2]. Using quasilinear analysis, significant wave-particle interaction between energetic ions and lower hybrid (LH) waves has been indeed demonstrated to occur [6, 7].

In a recent paper we have investigated the transition between cases in which one coherent LH wave is present in the system, with amplitude below the stochasticity threshold, and cases with the presence of several LH waves of close frequencies, studying the appearance of stochasticity along this transition [8]. We have employed a generalization of Karney's approach, assuming that a finite number of waves is present in the system, forming a sufficiently narrow wave packet in $\mathbf{k}$ space [8]. Despite the relative simplicity of the Hamiltonian obtained, the system dynamics has been shown to be complicated, originating interesting behavior which had not until quite recently been widely studied in the literature [9].

The analysis made in Ref. [8] has shown that in the particular case of a set of coherent waves the threshold for stochastic diffusion is reduced in comparison with the threshold in the one wave case, with the ensuing particle diffusion in velocity space occurring in periodic bursts along the time evolution. For a set of waves with random phases, the results appearing in Ref. [8] have shown more efficient long term diffusion in velocity space than in the case of the same number of coherent waves, although the initial diffusion rate for incoherent waves may be smaller than in the case of coherent waves. Reduction of the stochasticity threshold regarding the coherent one-wave case has also been obtained in other situations, for instance assuming two waves propagating obliquely to the ambient magnetic field [9], or considering the possibility of a modulation in the wave frequency [10].

In the present paper we resume the use of the theoretical approach employed in Ref. [8], now applied to the case of a finite set of waves with randomly chosen phases that are modified along time evolution. This procedure tends to average out all possibly remaining regularity in the distribution of the wave phases, so that the outcome must be close to that expected for a continuous wave packet.

The structure of the paper is the following. In Sec. 2 we present a summary of the theoretical formalism developed in Ref. [8], which helps to explain fundamental features of the system and show how to obtain the equations of motion. In Sec. 3 we present some numerical results which illustrate the appearance of stochastic diffusion in the system due to the presence of a set of incoherent lower hybrid waves, considering both the case of waves with random phases which are fixed along time evolution, and waves with random phases which change along the time evolution of the system. Finally, in Sec. 4 we summarize our findings and comment on the main results of the paper.

2 The description of the system and the equations of motion

Let us therefore consider the following magnetized system:

$$\mathbf{B} = B_0 \mathbf{e}_z$$

$$\mathbf{E} = \sum_i E_i(\omega_i) \cos\left(k_i(w_i) y - \omega_i t - \phi_i\right) \mathbf{e}_y. \qquad (1)$$

The ω_i appearing in this expression are angular frequencies of the individual waves in a set of n_ω waves, the $E_i(\omega_i)$ are the amplitudes of these waves, and the ϕ_i are their phases.

Assuming the Coulomb gauge,

$$\mathbf{A} = -B_0 y \mathbf{e}_x,$$

we can write $\mathbf{E} = -\nabla\Phi$, with

$$\Phi = -\sum_i \frac{E_i(\omega_i)}{k_i(\omega_i)} \sin\left(k_i(w_i)y - \omega_i t - \phi_i\right) \mathbf{e}_y. \qquad (2)$$

The Hamiltonian for the system can be written as follows.

$$h = \frac{P^2}{2m} + q\Phi, \qquad (3)$$

where

$$P^2 = p_x^2 + p_y^2 + q^2 B_0^2 y^2 - 2q p_x B_0 y,$$

and where q and m are the ion charge and mass respectively, and the p_i are the cartesian components of the particle momentum. We have used $p_z(t = 0) = 0$, which implies $p_z(t) = 0$.

For the sake of simplicity, we consider that n_ω is an odd number, with waves equally spaced in frequency. We denote the amplitude, the angular frequency and the phases of the central wave as $\overline{E}$, $\overline{\omega}$, and $\overline{\phi}$, respectively, and assume initial conditions such that the phase of the central wave is zero ($\overline{\phi} = 0$). Using these definitions, we introduce the dimensionless variables

$$t' = \Omega\, t, \quad \Omega = \frac{qB_0}{m}, \quad y' = \overline{k}\, y,$$

$$p_i' = \frac{\overline{k}}{m\Omega} p_i, \quad (i = x, y) \qquad (4)$$

where $\overline{k} = k_i(\omega_i = \overline{\omega})$.

As a consequence of these definitions, the Hamiltonian appears as follows.

$$h' = \frac{1}{2}\left[\left(p_x' + y'\right)^2 + p_y'^2\right]$$

$$-\alpha \sum_i \frac{r_{E_i}}{r_{k_i}} \sin\left(r_{k_i} y' - \nu_i t' - \phi_i\right), \qquad (5)$$

where

$$\alpha = \frac{qmE_0}{\overline{k}} \frac{\overline{k}^2}{m^2\Omega^2} = \frac{E_0}{B_0}\frac{\overline{k}}{\Omega} = \frac{E_0/B_0}{\Omega/\overline{k}},$$

$$r_{E_i} = \frac{E_i(\omega_i)}{E_0},$$

$r_{k_i} = k_i/\overline{k}$, $\nu_i = \omega_i/\Omega$, and $h' = hm/(m\Omega/\overline{k})^2$. The amplitude E_0 is obtained from the following normalization condition,

$$E_0^2 = 2\left\langle \left(\sum_i E_i \cos\varphi_i \mathbf{e}_y\right) \cdot \left(\sum_j E_j \cos\varphi_j \mathbf{e}_y\right) \right\rangle,$$

where $\varphi_i \equiv (k_i y - \omega_i t - \phi_i)$, and the symbol $< ... >$ means the time average over a time interval sufficiently large in order to be an integer multiple of the periods of all waves appearing in the $\mathbf{k}$ wave packet. The rate of amplitudes r_{E_i}, therefore satisfies the following constraint

$$\sum_{i=1}^{n_\omega} r_{E_i}^2 \left\langle \cos^2\varphi_i \right\rangle + 2 \sum_{i=1}^{n_\omega - 1} \sum_{j>i} r_{E_i} r_{E_j} \left\langle \cos\varphi_i \cos\varphi_j \right\rangle = \frac{1}{2}. \qquad (6)$$

After performing the time average, we obtain $\left\langle \cos^2\varphi_i \right\rangle = 0.5$, and $\left\langle \cos\varphi_i \cos\varphi_j \right\rangle = 0.0$, and therefore, from Eq. (6),

$$\sum_{i=1}^{n_\omega} r_{E_i}^2 = 1. \qquad (7)$$

Also for the sake of simplicity, we consider the case in which the n_ω waves of the $\mathbf{k}$ space packet have the same amplitude ($r_{E_i} = r_E$, for any i),

$$r_E = (n_\omega)^{-1/2}. \qquad (8)$$

We can also define $r_{\omega_i} = \omega_i/\overline{\omega}$, and consider that the wave spectrum is non-vanishing only between $\overline{\omega} - \delta\omega$ and $\overline{\omega} + \delta\omega$, and therefore r_{ω_i} spreads from $r_{\omega_i} = 1 - \Delta$ to $r_{\omega_i} = 1 + \Delta$, where $\Delta = \delta\omega/\overline{\omega}$. If the wave packet in $\mathbf{k}$ space is narrow, we may assume also for the sake of simplicity that for the waves in the packet

$$\frac{\omega}{k} \simeq V, \qquad (9)$$

where V is a constant. As a consequence,

$$r_{\omega_i} = \frac{\omega_i}{\overline{\omega}} = \frac{V k_i(\omega_i)}{V k_i(\overline{\omega})} = \frac{k_i(\omega_i)}{\overline{k}} = r_{k_i}(\omega_i),$$

and therefore

$$\nu_i = \frac{\omega_i}{\overline{\omega}}\frac{\overline{\omega}}{\Omega} = r_{k_i}\overline{\nu}, \quad \text{where} \quad \overline{\nu} = \frac{\overline{\omega}}{\Omega}.$$

Dropping the 'primes', for simplicity, we obtain as the system's Hamiltonian,

$$h = \frac{1}{2}\left[\left(p_x + y\right)^2 + p_y^2\right]$$

$$-\alpha \sum_i \frac{r_{E_i}}{r_{k_i}} \sin\left[r_{k_i}\left(y - \overline{\nu}t - \phi_i\right)\right]. \qquad (10)$$

Following steps similar to those employed in Ref. [1], we perform the following canonical transformation

$$(x, y, p_x, p_y) \Rightarrow (X, Y, P_x, P_y)$$

$$F_2(x, y, P_x, P_y) = (P_x - \overline{\nu}t)x + P_y(y - \overline{\nu}t + P_x) \qquad (11)$$

$$X = \frac{\partial F_2}{\partial P_x} = x + P_y$$

$$Y = \frac{\partial F_2}{\partial P_y} = y - \overline{\nu}t + P_x$$

$$p_x = \frac{\partial F_2}{\partial x} = P_x - \overline{\nu}t$$

$$p_y = \frac{\partial F_2}{\partial y} = P_y$$

$$K = h + \frac{\partial F_2}{\partial t} = h - \overline{\nu}(x + P_y) = h - \overline{\nu}X,$$

resulting

$$Y = y + p_x, \quad X = x + p_y.$$

The new Hamiltonian is

$$K(X, Y, P_x, P_y) = \frac{1}{2}\left[Y^2 + P_y^2\right]$$

$$-\alpha \sum_i \frac{r_{E_i}}{r_{k_i}} \sin\left[r_{k_i}(Y - P_x) - \phi_i\right] - \overline{\nu}X. \qquad (12)$$

Performing now a second canonical transformation,

$$(X, Y, P_x, P_y) \Rightarrow (I_1, \omega_1, I_2, \omega_2)$$

$$F_1(X, Y, \omega_1, \omega_2) = \frac{1}{2}Y^2 \text{cotg}(\omega_1) + X\omega_2.$$

$$P_x = \frac{\partial F_1}{\partial X} = \omega_2,$$

$$P_y = \frac{\partial F_1}{\partial Y} = Y\text{cotg}(\omega_1) \rightarrow P_y = (2I_1)^{1/2}\cos(\omega_1),$$

$$I_1 = -\frac{\partial F_1}{\partial \omega_1} = \frac{1}{2}Y^2 \text{cosec}^2(\omega_1) \rightarrow Y = (2I_1)^{1/2}\sin(\omega_1),$$

$$I_2 = -\frac{\partial F_1}{\partial \omega_2} = -X,$$

we arrive at the final form of the Hamiltonian, denoted as H,

$$H = K + \frac{\partial F_1}{\partial t} = K.$$

The Hamiltonian is therefore

$$H = I_1 + \overline{\nu}I_2$$

$$-\alpha \sum_i \frac{r_{E_i}}{r_{\omega_i}} \sin\left\{r_{\omega_i}\left[R\sin(\omega_1) - \omega_2\right] - \phi_i\right\}, \qquad (13)$$

where we have used $r_{k_i} = r_{\omega_i}$ and defined $R = (2I_1)^{1/2}$.

The Hamiltonian equations are easily obtained as follows

$$\dot{\omega}_i = \frac{\partial H}{\partial I_i}, \quad \dot{I}_i = -\frac{\partial H}{\partial \omega_i},$$

$$\dot{\omega}_1 = 1 - \sin(\omega_1)\frac{1}{R}\alpha \sum_i r_{E_i} \cos\left\{r_{\omega_i}\left[R\sin(\omega_1) - \omega_2\right] - \phi_i\right\},$$

$$\dot{\omega}_2 = \overline{\nu},$$

$$\dot{I}_1 = \cos(\omega_1)R\alpha \sum_i r_{E_i} \cos\left\{r_{\omega_i}\left[R\sin(\omega_1) - \omega_2\right] - \phi_i\right\},$$

$$\dot{I}_2 = -\alpha \sum_i r_{E_i} \cos\left\{r_{\omega_i}\left[R\sin(\omega_1) - \omega_2\right] - \phi_i\right\}. \qquad (14)$$

This set of coupled equations is now ready to be object of a numerical analysis, with results presented in Sec. 3.

3 Some numerical results

For the numerical solution of the Hamiltonian equations, we assume a given number of particles (n_p) and a given number of waves (n_ω) and give α and $\overline{\nu}$ as parameters. We also assume a given value of Δ and a distribution of wave amplitudes r_{E_i}.

As loading procedure for the numerical calculation we initially consider the following case: We give parameters I_1^0, a_0, and the initial Hamiltonian H, and attribute, for the n_p particles, regularly spaced values of I_1, ω_1 and ω_2:

$$I_1 = I_1^0 + \frac{1}{n_p}a_0, I_1^0 + \frac{2}{n_p}a_0, ..., I_1^0 + a_0,$$

$$\omega_1 = 2\pi\frac{1}{n_p}, 2\pi\frac{2}{n_p}, ..., 2\pi,$$

$$\omega_2 = 2\pi\frac{1}{n_p}, 2\pi\frac{2}{n_p}, ..., 2\pi,$$

$$I_2 = (H - I_1 + S)/\overline{\nu}, \qquad (15)$$

where

$$S \equiv \alpha \sum_i \frac{r_{E_i}}{r_{\omega_i}} \sin\left\{r_{\omega_i}\left[R\sin(\omega_1) - \omega_2\right] - \phi_i\right\}.$$

In other words, the loading procedure assumes initial values for I_1, ω_1 and ω_2, and evaluate I_2, in such a way that all the particles have the same initial Hamiltonian (H), for which we have arbitrarily assumed the value $H = I_1^0 + \overline{\nu}I_1^0$.

In Ref. [8] we have also considered the same set of particle initial conditions utilized here, and also a different set of initial conditions. The results obtained were qualitatively similar in both cases, indicating that they were not restricted to a special set of conditions.

It is useful to remark here that when assuming the initial value of I_1 for each particle, we are simply assuming the initial value of the perpendicular canonical momentum of the particles, since reversing the canonical transformations one obtains

$$I_1 = \frac{1}{2}\frac{\overline{k}^2}{m^2\Omega^2}\left[p_y^2 + (p_x - qA_x)^2\right],$$

where p_x and p_y are the x and y dimensional components of the particle momentum, as used in Eq. (3), before the introduction of the dimensionless variables by Eq. (4).

With the choice of parameters I_1^0 and a_0, the spread of perpendicular momenta of the particles is such that $50.0 < R < 57.4$, where as we have seen $R = \sqrt{2I_1}$. This range of parameters is similar to that utilized in previous studies of the one-wave case, which we use for comparison when considering the case of several waves [1, 2].

According to these studies, for one wave and integer value of $\overline{\nu}$, and small wave amplitude, the phase space is dominated by large first order islands. At intermediate wave amplitudes, stochastic motion appears near the separatrixes between the islands. For growing wave amplitude the size of the stochastic region increases, and the threshold for stochasticity has been defined as the wave amplitude for which the fraction of phase space occupied by the islands has appreciably diminished, in comparison with the size of stochastic regions [1]. The limits of the stochastic region are

α dependent and have been stablished approximately as the following [1],

$$R_{min} = \overline{\nu} - \sqrt{\alpha}, \quad R_{max} = (4\alpha\overline{\nu})^{2/3}(2/\pi)^{1/3}.$$

For $\overline{\nu} = 30$ and $\alpha = 2.0$, the stochasticity therefore will fully occur in the region $28.6 < R < 33.2$. For $\alpha = 4.0$, in the region $28.0 < R < 43.5$, and for $\alpha = 6.0$, in the region $27.5 < R < 69.0$. Therefore, for our choice of parameters, in the one-wave case small amount of stochasticity may be expected for $\alpha = 2.0$, for instance, since the range $50.0 < R < 57.4$ is far from the stochastic range, and appreciable amount of stochasticity for $\alpha = 4.0$, since the range $50.0 < R < 57.4$ is close to the stochastic range. On the other hand, for larger wave amplitude, as in the case of $\alpha = 6.0$, for instance, one can expect fully stablished stochasticity in the chosen range, which will be completely immersed in the stochastic region. These expectations will be now subjected to numerical confirmation, and compared to the case of fixed wave amplitude and different number of incoherent waves.

We start by considering the one-wave case, same situation considered in Refs. [1] and [2].

In order to illustrate the effect of the increase of the wave intensity, we present in Fig. 1 the quantity R versus ω_2 (mod. 2π), for the case of 50 particles and one wave, with $\alpha = 2.0$, 3.0, 4.0, and 5.0, assuming $I_1^0 = 1.25 \times 10^3$, $a_0 = 400$, and $\overline{\nu} = 30.0$. The sequence of panels illustrates the gradual modification of particle trajectories caused by the increase in the wave intensity. It is seen the gradual appearance of the overlap of particle orbits which has been shown to correspond to stochastic diffusion in velocity space [1, 2].

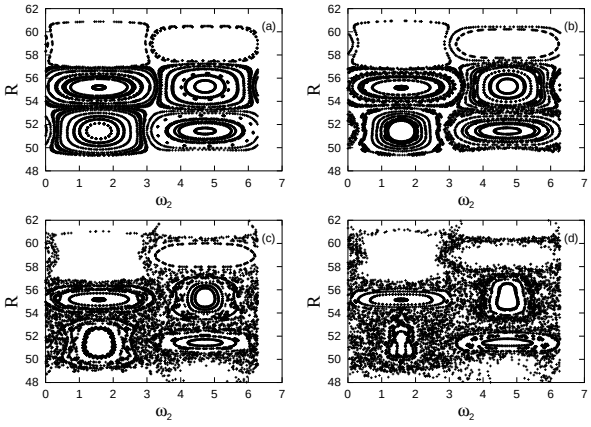

Figure 1. R as a function of ω_2 (mod. 2π), for 50 particles, one wave ($n_\omega = 1$), $\overline{\nu} = 30$, and (a) α= 2.0, (b) α=3.0, (c) $\alpha = 4.0$, and (d) $\alpha = 5.0$.

We now consider the presence of more than one wave, with different frequencies and random phases which are fixed in time, with the phase of the central wave assumed to be zero ($\overline{\phi} = 0$). The random phases are obtained from a random number generator which starts from a numerical seed. All the results which follow, unless explicitly stated otherwise, are generated with the use of the same seed for the random number generator.

In Fig. 2 it is seen the case of R versus ω_2 (mod. 2π), considering 50 particles and $\alpha = 2.0$, for several values of the number of waves (1, 3, 5, and 7), using $\Delta = 1.0 \times 10^{-2}$ and the other parameters as in Fig. 1. Figure 2 clearly shows that the presence of the waves with random phases cause the complete spreading of the particle orbits which are present in the case of only one-wave, for the same value of α.

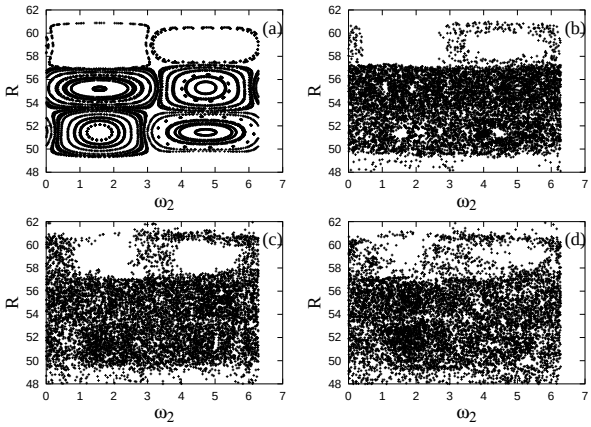

Figure 2. R as a function of ω_2 (mod. 2π), for 50 particles and waves with fixed random phases, α= 2.0, $\overline{\nu} = 30$, $\Delta = 1.0 \times 10^{-2}$, and number of waves (a) 1, (b) 3, (c) 5, and (d) 7.

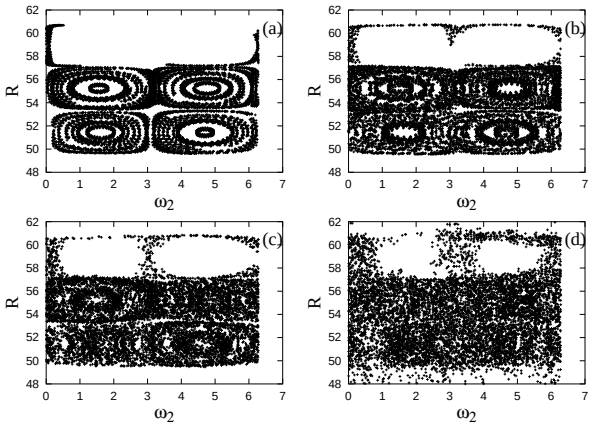

Figure 3. R as a function of ω_2 (mod. 2π), for 50 particles and waves with fixed random phases, $\Delta = 1.0 \times 10^{-2}$, $n_\omega = 5$, and (a) α= 0.25, (b) α= 0.5, (c) α= 1.0, and (d) α= 2.0.

In Fig. 3 we show R as a function of ω_2 (mod. 2π), for the case in which five waves are present in the system, considering smaller values of the wave amplitude ($\alpha = 0.25, 0.5, 1.0$, and 2.0), and $\Delta = 1.0 \times 10^{-2}$, and waves with random phases. The loading procedure and other parameters are also the same as in the previous figures. We observe that the amount of stochastic diffusion, for the same number of iterations, gradually decreases when the wave energy is reduced, but even in the case of α= 0.25 the degree of stochasticity is larger than that obtained in the one-wave case and α= 2.0, seen in the first panel of Fig. 1 and in the first panel of Fig. 2.

The presence of stochastic behavior can also be investigated by following the time behavior of the following quantities,

$$(\delta I_j)_t = \left\{ \frac{1}{n_p - 1} \sum_{i=1}^{n_p} \left[I_j(t) - I_j(0) \right]^2 \right\}^{1/2} , \qquad (16)$$

where $j = 1, 2$. In a plot of $(\delta I_j)_t$ versus t, the inclination of $(\delta I_j)_t$ relative to the t axis is a measure of the diffusion coefficient in velocity space [11].

In Fig. 4 we show $(\delta I_1)_t$ as a function of normalized time, for $I_1^0 = 1.25 \times 10^3$, $a_0 = 400$, $\overline{\nu} = 30.0$, and $\alpha = 2.0$, for n_ω= 1, 5, and 9, for the case of waves with random phases which are fixed in time. For this figure, we have considered $n_p = 1000$, which results in much better statistics than obtained with $n_p = 50$. The Poincaré plots presented in Figs. 1 to 3, on the other hand, were obtained with $n_p = 50$ because with a larger number of particles it becomes very difficult to see any structure in the plots, due to the proximity of the dots which represent sucessive passages of particles by the Poincaré section. Panel (a) shows the evolution up to $t \simeq 120$, while panel (b) shows the evolution up to $t \simeq 1200$. According to Fig. 4, the long term evolution of the quantity $(\delta I_1)_t$ appearing in Fig. 4b shows continued diffusion, without the conspicuous "steps" appearing in the case of coherent waves [8].

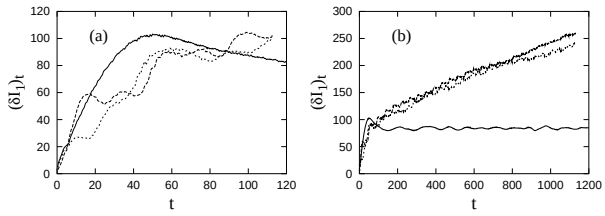

Figure 4. $(\delta I_1)_t$ as a function of normalized time, for the case of waves with fixed random phases, for $I_1^0 = 1.25 \times 10^3$, $a_0 = 400$, $\overline{\nu} = 30.0$, and $\alpha = 2.0$, for n_ω= 1 (full line), 5 (broken line), and 9 (dotted line). (a) Short-term evolution; (b) Long-term evolution.

Figure 4 has been obtained for a given set of random phases. If a different seed would be attributed to the random number generator, a different set of random phases would be obtained, which would result in different time evolution for the quantity depicted in the figure. We have obtained results for different sets of initial random phases, some of which have been displayed in Ref. [8]. What we have observed from these different cases is that, although the obvious differences between the different curves obtained, the inclination relative to the t axis is approximately the same in all corresponding cases, indicating similar average diffusive behavior. The interesting parameters for the emulation of the interaction of a narrow wave packet with energetic particles seem to be the wave energy and the width of the spectrum, and not the particular phases of the waves composing the finite set of waves chosen to arbitrarily represent the spectrum. These results could be in principle improved by an ensemble average, considering a large number of sets of random phases, which would require very intensive use of numerical calculation. It is expected that the average behavior obtained using different sets of random phases would tend to become more and more similar for increasing number of waves, so that in the limit of infinite wave number the difusion caused by the waves would be independent of the particular set of random phases utilized in the calculation. Instead of proceeding with this costly approach, we may consider the case of a finite set of waves, with randomly chosen phases that are modified along time evolution, which tend to average out all possibly remaining regularity in the phase distribution, so that the outcome must be close to that expected for a continuous wave packet.

We now consider the presence of more than one wave, with different frequencies and random phases which are modified along the time evolution, with the initial phase of the central wave assumed to be zero ($\overline{\phi} = 0$). The phases are modified after a real time interval which averages $\delta t = 2\pi/\delta\omega$, so that for longer time intervals all phase correlations are averaged out. In nondimensional time, for $\Delta = 1.0 \times 10^{-2}$ and $\overline{\nu} = 30.0$, the modification of the phases occurs after an average interval $\delta t \simeq 20$. The effect of the finite set of waves becomes truly random and more adequate to the emulation of a wave packet of finite width.

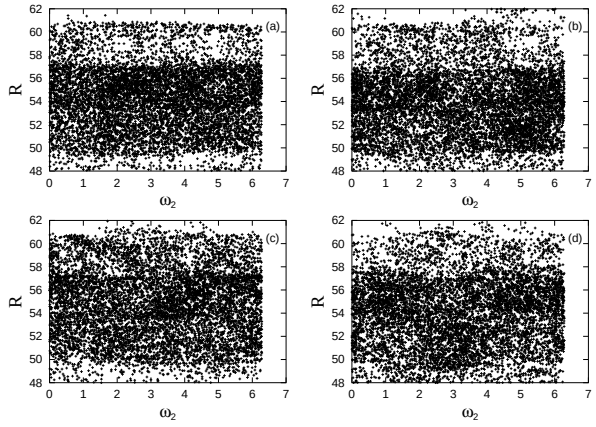

Figure 5. R as a function of ω_2 (mod. 2π), for 50 particles and waves with random phases which change along time evolution, α= 2.0, $\overline{\nu} = 30$, $\Delta = 1.0 \times 10^{-2}$, and number of waves (a) 1, (b) 3, (c) 5, and (d) 7.

For this situation, in Fig. 5 it is seen the Poincaré plot of R versus ω_2 (mod. 2π), again considering 50 particles and $\alpha = 2.0$, for several values of the number of waves (1, 3, 5, and 7), using $\Delta = 1.0 \times 10^{-2}$ and the other parameters as in Fig. 1. Except for the random phases which change along time, these are exactly the same conditions used to generate Fig. 2. Fig. 5 clearly shows that the randomly changing phases cause the complete spreading of the particle orbits which appeared in the fixed phase one-wave case, resulting in a plot which appears qualitatively independent of the number of the waves, at least for the region in phase space which is depicted in Fig. 5.

In Fig. 6 we show R as a function of ω_2 (mod. 2π), for the case in which five waves with randomly changing phases are present in the system, considering smaller values of the

wave amplitude ($\alpha = 0.25, 0.5, 1.0,$ and 2.0, the same values considered for Fig. 3), and $\Delta = 1.0 \times 10^{-2}$. The loading procedure and other parameters are also the same. We observe that the amount of stochastic diffusion, for the same number of iterations, is gradually smaller for smaller wave energy, but even in the case of α= 0.25 the degree of stochasticity is larger than that obtained in the one-wave case and α= 2.0, seen in the first panel of Fig. 1 and in the first panel of Fig. 2. Comparing the first panel of Fig. 6 with the first panel of Fig. 3, it is seen that the randomness of the phases is responsible for significant diffusive behavior which was pratically absent in the corresponding case of $\alpha = 0.25$ for five waves with fixed phases.

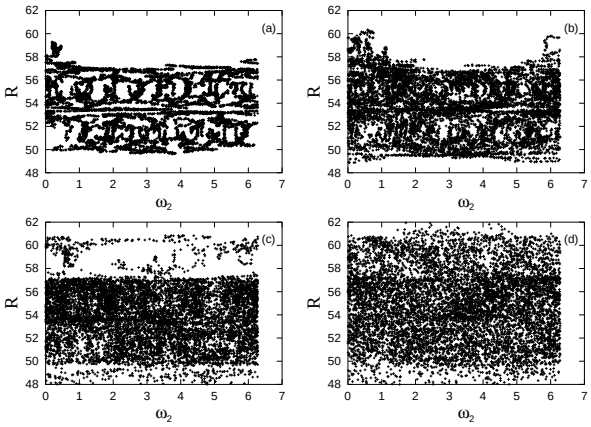

Figure 6. R as a function of ω_2 (mod. 2π), for 50 particles and waves with random phases which change along time evolution, $\Delta = 1.0 \times 10^{-2}$, $n_\omega = 5$, and (a) α= 0.25, (b) α= 0.5, (c) α= 1.0, and (d) α= 2.0.

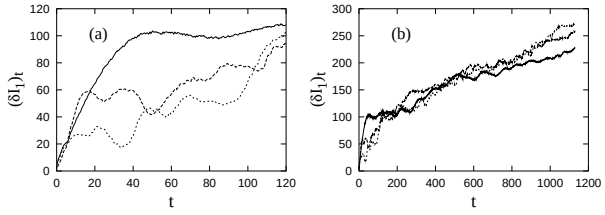

Figure 7. $(\delta I_1)_t$ as a function of normalized time, for the case of waves with random phases that change along time evolution, for $I_1^0 = 1.25 \times 10^3$, $a_0 = 400$, $\overline{\nu} = 30.0$, and $\alpha = 2.0$, for n_ω= 1 (full line), 5 (broken line), and 9 (dotted line). (a) Short-term evolution; (b) Long-term evolution.

Proceeding along the proposed line, in Fig. 7 we show $(\delta I_1)_t$ as a function of normalized time, for $I_1^0 = 1.25 \times 10^3$, $a_0 = 400$, $\overline{\nu} = 30.0$, and $\alpha = 2.0$, for n_ω= 1, 5, and 9, for the case of waves with random phases that change along time evolution. As for Fig. 4, the number of particles has been assumed to be 1000. The long-term evolution depicted at panel (b) at the right-hand side shows that the stochasticity introduced by the randomly changing waves results in continued diffusive behavior in velocity space, even for the one wave case.

In Fig. 8 we show $(\delta I_1)_t$ as a function of normalized time, for the one-wave case ($n_\omega = 1$), $I_1^0 = 1.25 \times 10^3$, $a_0 = 400$, $\overline{\nu} = 30.0$, and α = 2.0, 3.0, 4.0, and 5.0, considering that the phase of the wave changes randomly along the time evolution. Panel (a) of Fig. 8 shows the evolution up to normalized $t \simeq 120$, and panel (b) shows the extended evolution, up to $t \simeq 1200$. Fig. 8 clearly shows that long-term diffusive behavior, measured by the inclination of the curve relative to the t axis, is nearly proportional to the wave amplitude, while it should be nearly absent in the region of the phase space depicted in the figure, for $\alpha \simeq 2.0$, if the phase of the wave were kept constant along time evolution, according to the analysis presented at the beginning of the present section.

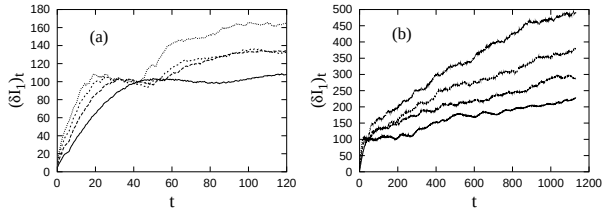

Figure 8. $(\delta I_1)_t$ as a function of normalized time, for $n_\omega = 1$, $I_1^0 = 1.25 \times 10^3$, $a_0 = 400$, $\overline{\nu} = 30.0$, and α = 2.0 (full line), 3.0 (broken line), 4.0 (dashed line), and 5.0 (dotted line). The phase of the wave is randomly modified along time evolution. (a) Short-term evolution; (b) Long-term evolution.

4 Final remarks

We have generalized the discussion on stochastic diffusion of energetic ions by lower hybrid waves by considering a case where a set of waves with similar frequencies and random phases which change randomly along time evolution is present in the system. As in Ref. [8], the task has been accomplished by generalization of the approach utilized in Refs. [1, 2] under the restriction that the spectra is sufficiently narrow such that the phase velocity of the waves present in the system can be considered to be a constant. The present discussion generalizes previous results obtained assuming a set of waveswith fixed phases, since the random modification of the phases along time evolution tends for long time evolution to be equivalent to an ensemble average over fixed phases, which would be much more costly from a numerical point of view.

The results obtained indicate significant long term diffusion which is nearly independent from the number of waves present in the system. The random modification of the phases along time evolution averages possible regularities originated from a given set of phases, and produces stochastic diffusion which must be close to that expected from a continuous wave packet of finite fequency width.

Acknowledgments

The authors acknowledge support by the Brazilian agencies Conselho Nacional de Desenvolvimento Científico e Tecnológico (CNPq) and Fundação de Amparo à Pesquisa do Estado do Rio Grande do Sul (FAPERGS). Useful comments by I. L. Caldas, Ricardo L. Viana and R. R. B. Correa are gladly acknowledged.

References

[1] C. F. F. Karney, Phys. Fluids **21**, 1584 (1978).

[2] C. F. F. Karney, Phys. Fluids **22**, 2188 (1979).

[3] M. C. R. de Andrade, M. Brusati, and the JET team, Plasma Phys. Contr. Fusion **36**, 1171 (1994).

[4] D. Testa *et al.*, Plasma Phys. Contr. Fusion **41**, 507 (1999).

[5] L. F. Ziebell and L. M. Tozawa, Braz. J. Phys. **28**, 222 (1998).

[6] L. M. Tozawa and L. F. Ziebell, Braz. J. Phys. **28**, 211 (1998).

[7] L. F. Ziebell, Plasma Phys. Contr. Fusion **42**, 359 (2000).

[8] L. M. Tozawa and L. F. Ziebell, Phys. Rev. E **66**, 056409, 13p. (2002).

[9] S. Benkadda, A. Sen, and D. R. Shklyar, Chaos **6**, 451 (1996).

[10] S. Riyopoulos, Phys. Fluids **28**, 1097 (1985).

[11] D. Farina, R. Pozzoli, and M. Romé, Phys. Plasmas **1**, 1871 (1994).